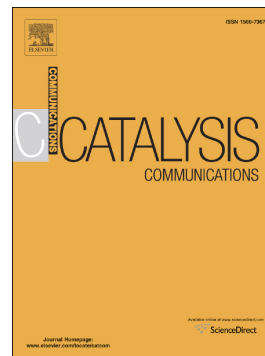


## Journal Pre-proof

Enhanced reduction of nitrobenzene derivatives: Effective strategy executed by Fe<sub>3</sub>O<sub>4</sub>/PVA-10%Ag as a versatile hybrid nanocatalyst

Jamal Rahimi, Reza Taheri-Ledari, Maryam Niksefat, Ali Maleki



PII: S1566-7367(19)30311-5

DOI: <https://doi.org/10.1016/j.catcom.2019.105850>

Reference: CATCOM 105850

To appear in: *Catalysis Communications*

Received date: 20 July 2019

Revised date: 14 October 2019

Accepted date: 15 October 2019

Please cite this article as: J. Rahimi, R. Taheri-Ledari, M. Niksefat, et al., Enhanced reduction of nitrobenzene derivatives: Effective strategy executed by Fe<sub>3</sub>O<sub>4</sub>/PVA-10%Ag as a versatile hybrid nanocatalyst, *Catalysis Communications* (2018), <https://doi.org/10.1016/j.catcom.2019.105850>

This is a PDF file of an article that has undergone enhancements after acceptance, such as the addition of a cover page and metadata, and formatting for readability, but it is not yet the definitive version of record. This version will undergo additional copyediting, typesetting and review before it is published in its final form, but we are providing this version to give early visibility of the article. Please note that, during the production process, errors may be discovered which could affect the content, and all legal disclaimers that apply to the journal pertain.

© 2018 Published by Elsevier.

**Enhanced reduction of nitrobenzene derivatives: Effective strategy executed by Fe<sub>3</sub>O<sub>4</sub>/PVA-10%Ag as a versatile hybrid nanocatalyst**

Jamal Rahimi, Reza Taheri-Ledari, Maryam Niksefat, Ali Maleki\*

*Catalysts and Organic Synthesis Research Laboratory, Department of Chemistry, Iran University of Science and Technology, Tehran 16846-13114, Iran*

*\*Corresponding author. Tel.: +98 21 73228313; fax: +98 21 73021584. E-mail address: maleki@iust.ac.ir (A. Maleki).*

---

**Abstract**

Herein, we present an organic–inorganic hybrid nanocomposite constructed of polyvinyl alcohol (PVA), iron oxide (Fe<sub>3</sub>O<sub>4</sub>), and 10% of silver nanoparticles (Ag NPs). First, a convenient *in situ* method is introduced for the preparation of this efficient catalytic system (Fe<sub>3</sub>O<sub>4</sub>/PVA-10%Ag). Further, we study the high catalytic performance for the reduction of nitrobenzene (NB) derivatives as a hazardous species of chemicals and the significant biological activity (antibacterial effects) of the nanocomposite. However, high reaction yields (99%) have been obtained in short reaction times (~15 min). A plausible mechanism is suggested, and all the required characterizations of the presented nanocatalyst are investigated in this study.

**Keywords:** Hybrid magnetic nanocomposite; Hazardous materials; Effective electronic interactions; Nitrobenzene derivatives; Polyvinyl alcohol.

---

## 1. Introduction

In the field of environmental studies, removal of contaminants from the natural resources has become a serious concern and attracted much attention [1]. Proportional to increasing industrial activities and discharge of the waste into the water resources, this concern has become more intense in the last decade [2]. Among various hazardous species of the aqueous pollutants, nitrobenzene (NB), which results from industrial sources such as pharmaceuticals, agrochemicals, and dyes, is noted for its toxicity, carcinogenicity, and persistence [3-5]. One of the most convenient methods to deal with NB is the reduction of NB derivatives to anilines as nonhazardous compounds [6–10]. In this regard, several methods and tools have been reported by researchers to facilitate the reduction reaction of NB derivatives [3–11]. Among numerous efficient nanocatalysts, iron oxide ( $\text{Fe}_3\text{O}_4$ ) nanoparticles (NPs) have attracted increasing attention owing to their magnetic property, extreme surface area, surface-functionalization ability, notable thermal resistance, nontoxicity, and therapeutic properties [12–16]. Our research group has reported several works on these magnetic catalytic systems. Moreover, Mallakpour *et al.* have also reported an LDH-supported  $\text{Fe}_3\text{O}_4$ /PVA magnetic nanocomposite for the removal of methyl orange from aqueous solution [17]. As a continuation of our previous research, herein,  $\text{Fe}_3\text{O}_4$  NPs coated with PVA ( $\text{Fe}_3\text{O}_4$ /PVA) are decorated with silver nanoparticles (Ag NPs) and employed for the reduction of NB derivatives to anilines in the presence of hydrazine hydrate ( $\text{N}_2\text{H}_4\cdot\text{H}_2\text{O}$ ) [18–21]. Reduction of NB derivatives using  $\text{N}_2\text{H}_4\cdot\text{H}_2\text{O}$  in the presence of a nanoscale facilitator has been introduced as an efficient strategy. For example, this method has recently been implemented with  $\text{CeO}_2$  NPs, by Anbu *et al.* [22]. Noble metal-supported  $\text{Fe}_3\text{O}_4$  nanostructured materials have shown better activity owing to the synergistic effect between metal and metal oxides [23,24]. Nevertheless, PVA is typically used to modify the surface of  $\text{Fe}_3\text{O}_4$  NPs and increase hydroxyl groups onto the surface of the NPs. Through this method, more ratios of Ag NPs could be loaded onto the surface of PVA-coated NPs, and as a result, more active sites are obtained.

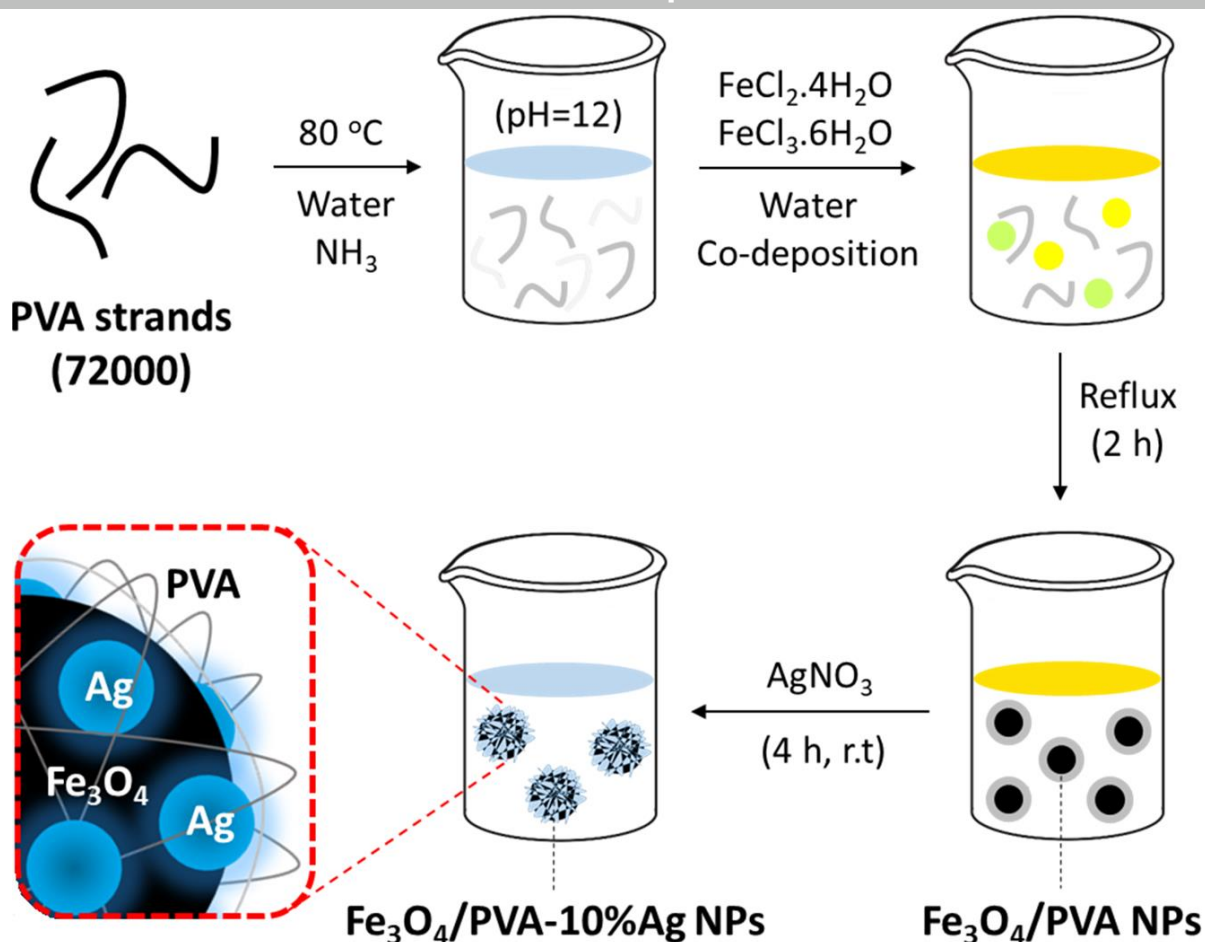
Herein, we present PVA-coated  $\text{Fe}_3\text{O}_4$  NPs decorated with Ag NPs with 9.94% weight ratio ( $\text{Fe}_3\text{O}_4$ /PVA-10%Ag) as an effective nanocatalyst for the reduction of the NB derivatives to anilines. A convenient separation process was carried out using an external magnet, through the magnetic

property of Fe<sub>3</sub>O<sub>4</sub>/PVA-10%Ag. The NB reduction reactions were precisely screened in the presence of N<sub>2</sub>H<sub>4</sub>.H<sub>2</sub>O and under mild conditions, and acceptable reaction yields were obtained during the short reaction times. Additionally, the catalyst reusability was monitored after recycling and using the catalyst several times. As the second application, the biological activity of Fe<sub>3</sub>O<sub>4</sub>/PVA-10%Ag was precisely investigated through the implementation of the antimicrobial tests.

## 2. Results and discussion

### 2.1. Preparation

PVA-coated Fe<sub>3</sub>O<sub>4</sub> NPs were prepared by an *in situ* co-deposition process in which PVA strands (72000) were well dissolved in deionized water at 80 °C until a homogeneous mixture was obtained. Then, NH<sub>3</sub> was added into the flask until pH~12 was attained. Afterward, the atmosphere of the reaction was neutralized using N<sub>2</sub> gas, and a clear yellow solution of FeCl<sub>2</sub>.4H<sub>2</sub>O and FeCl<sub>3</sub>.6H<sub>2</sub>O in deionized water was added drop wise into the flask. After conversion of the mixture to dark particles, stirring was continued for additional 2 h at 80 °C (reflux condition), and then, they were magnetically separated and washed several times with acetone and deionized water. The washed particles were dried at 60 °C in an oven, and powdered as fine particles by the ball milling process. At the second stage, the synthesized Fe<sub>3</sub>O<sub>4</sub>/PVA magnetic NPs were well dispersed in deionized water by ultrasonication (15 min), and then, silver nitrate was added, and the mixture was stirred for 4 h at room temperature. Ultimately, the produced dark brown particles were magnetically isolated from the mixture and washed several times with deionized water and dried at 60 °C in the oven (Scheme 1).



**Scheme 1.** Synthetic pathway of the  $\text{Fe}_3\text{O}_4/\text{PVA}-10\%\text{Ag}$  nanocomposite.

## 2.2. Characterization

For structural characterization studies of the fabricated  $\text{Fe}_3\text{O}_4/\text{PVA}-10\%\text{Ag}$  nanocomposite, both Fourier-transform infrared (FT-IR) spectroscopy and energy dispersive X-ray (EDX) spectroscopy were performed and the spectra were precisely investigated, as shown in Figure S1 in the Supplementary Information (SI) section. Elemental analysis on the desired product proved that all essential elements such as iron, carbon, oxygen, and silver were present in the structure of the  $\text{Fe}_3\text{O}_4/\text{PVA}-10\%\text{Ag}$  nanocomposite, and the quantitative ratio of each element is reported in Table S1 in the SI section. As shown in the table, the weight ratio of Ag NPs with a near approximation is considered 10%. The presence of the Ag NPs was also approved by X-ray photoelectron spectroscopy (XPS) (Figure S7). Figure S1b shows the FT-IR spectra of PVA-coated  $\text{Fe}_3\text{O}_4$  NPs and the  $\text{Fe}_3\text{O}_4/\text{PVA}-10\%\text{Ag}$  nanocomposite. The comprehensive interpretation of the peaks that appeared in

the FT-IR spectra has also been given in the SI section, which proves the well surface-functionalization of the magnetic NPs. To obtain more confirmation about the structure of the  $\text{Fe}_3\text{O}_4/\text{PVA-10\%Ag}$  nanocomposite, X-ray diffraction (XRD) pattern of the desired product was obtained and compared with the reference patterns of  $\text{Fe}_3\text{O}_4$  NPs and Ag NPs (Figure 1). The XRD patterns of  $\text{Fe}_3\text{O}_4$  MNPs and Ag NPs have been reported according to the database of *JCPDS* (PDF#99-0073) and (PDF#87-0597), respectively. As shown in the figure, the peaks that appeared at  $2\theta = \sim 30.7^\circ, 36.2^\circ, 43.8^\circ, 57.7^\circ,$  and  $63.4^\circ$  are related to the diffraction pattern of  $\text{Fe}_3\text{O}_4$  NPs (pattern a). They are highlighted as blue circles in the XRD pattern of the desired product (pattern c). They are also marked by their Miller indices (2 2 0), (3 1 1), (4 0 0), (5 1 1), and (4 4 0), respectively (pattern a). In addition, the peaks that appeared at  $2\theta = \sim 38.0^\circ, 44.2^\circ, 64.3^\circ,$  and  $77.2^\circ$  corresponded to the Ag NP diffraction pattern (pattern b). They are highlighted as red squares in the XRD pattern of the desired product. Additionally, they are marked by their Miller indices (1 1 1), (2 0 0), (2 2 0), and (3 1 1) (pattern b). As compared with two reference patterns (a,b), a new peak appeared at  $\sim 32.7^\circ$ , which has been marked as a star, was observed in the spectrum of the  $\text{Fe}_3\text{O}_4/\text{PVA-10\%Ag}$  nanocomposite. This new peak is attributed to the PVA strands that coated the magnetic core. The mean size of the  $\text{Fe}_3\text{O}_4/\text{PVA-10\%Ag}$  nanocomposite was also calculated as  $\sim 21$  nm using HighScore Plus software and Debye-Scherrer formula.

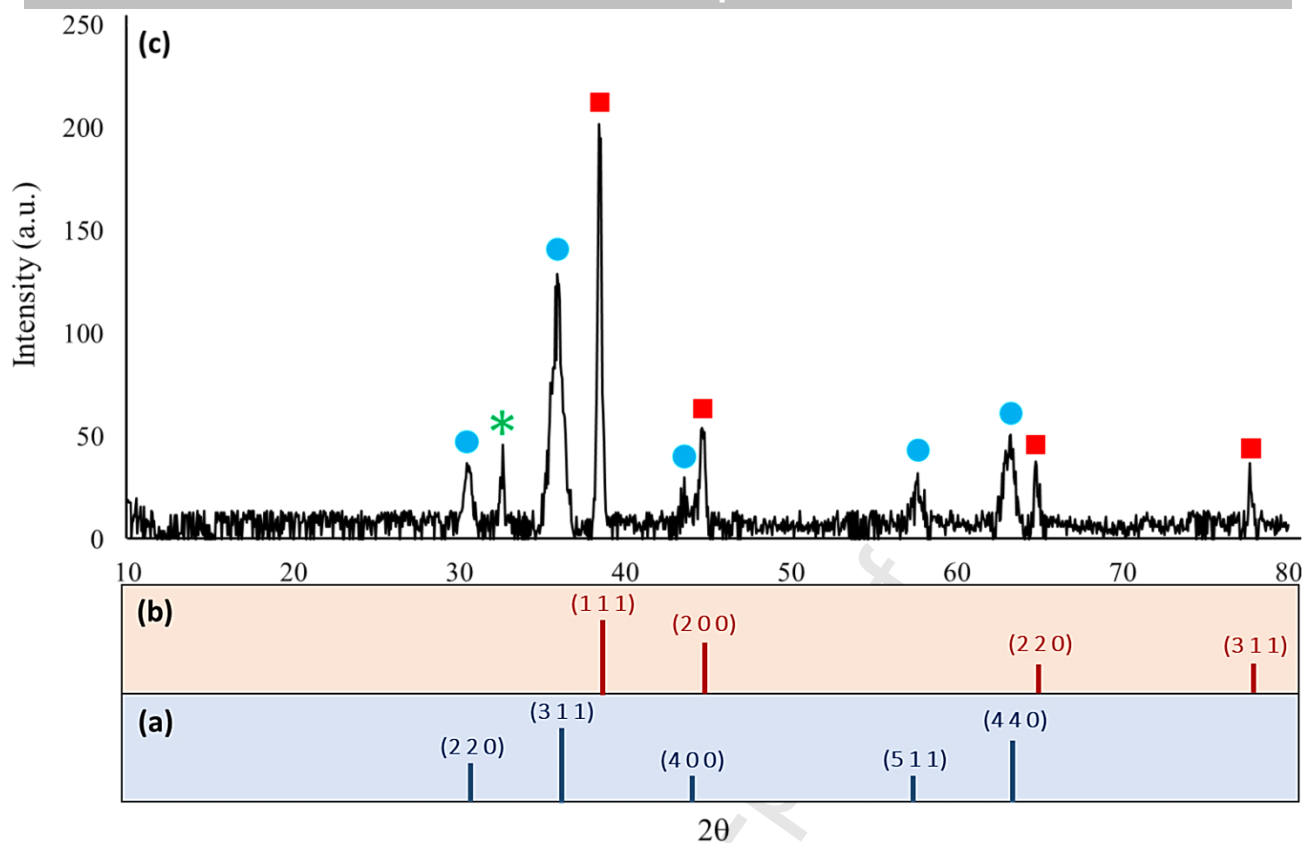


**Figure 1.** XRD patterns of (a)  $\text{Fe}_3\text{O}_4$  NPs; (b) Ag NPs; and (c)  $\text{Fe}_3\text{O}_4/\text{PVA}-10\%\text{Ag}$  nanocomposite; ( $\square$ ): new peak, ( $\bullet$ ): peak related to  $\text{Fe}_3\text{O}_4$  NPs, and ( $\blacksquare$ ): peak related to Ag NPs.

Microscopic images of the desired product were also captured using a scanning electron microscope (SEM), and the results of the morphology and size of the NPs were precisely investigated. As shown in Figure 2, the uniform spherical NPs collectively were fabricated during the *in situ* process. However, agglomeration was also observed in some places of the sample, which probably occurred because of the swelling and shrinkage property of the PVA polymeric network and the superparamagnetic behavior of the nanocomposite. The SEM images of the  $\text{Fe}_3\text{O}_4/\text{PVA}-10\%\text{Ag}$  nanocomposite revealed the particle size. The statistical data of particle sizes (for 30 particles) revealed that the mean size is  $20 \pm 15$  nm, and this value completely corresponded to the obtained value from the XRD study. Moreover, some of the brilliant spots in the image (a) were most likely related to the Ag NPs onto the surface of  $\text{Fe}_3\text{O}_4$  NPs. The TEM images are illustrated in Figure S8 (SI section), and they show well distribution of the Ag NPs onto and between the PVA textures.

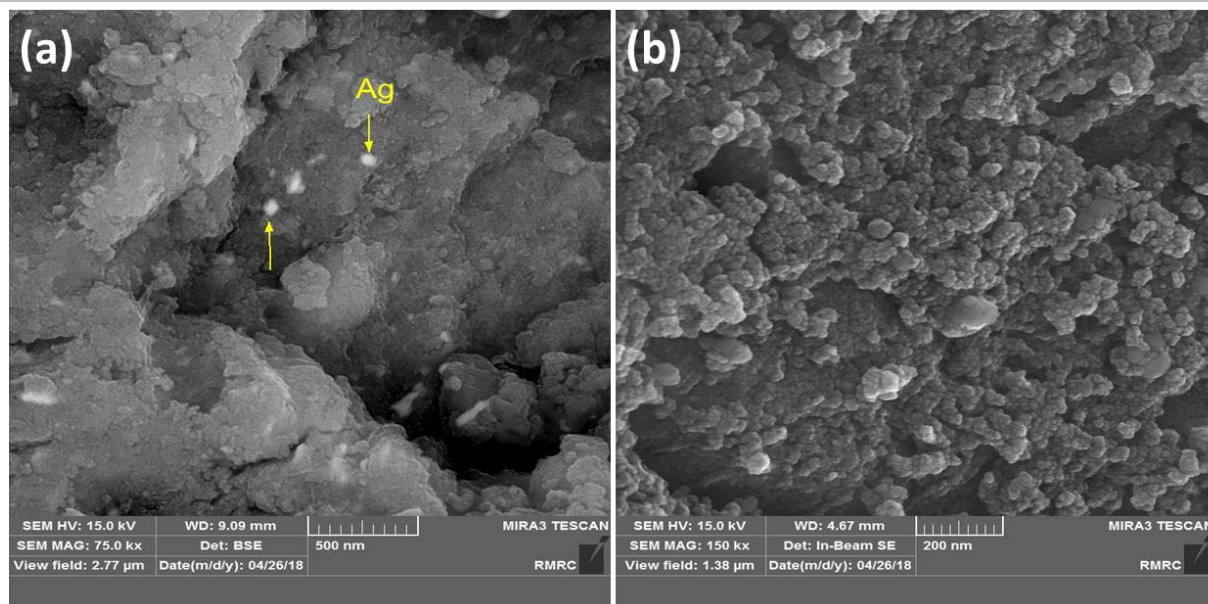


**Figure 2.** SEM images of the Fe<sub>3</sub>O<sub>4</sub>/PVA-10%Ag nanocomposite.

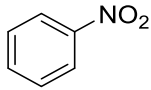
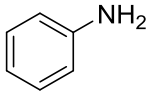
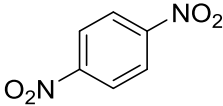
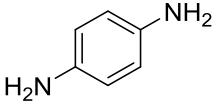
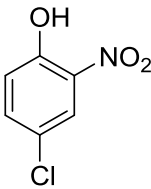
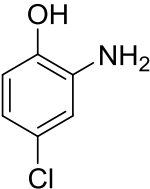
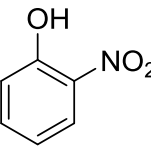
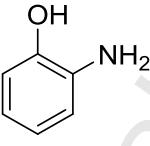
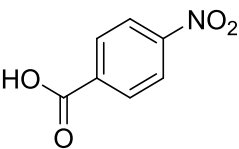
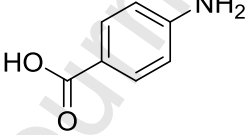
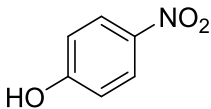
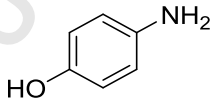
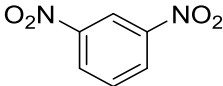
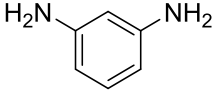
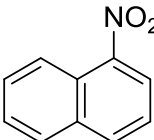
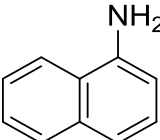
The thermal behavior of the fabricated Fe<sub>3</sub>O<sub>4</sub>/PVA-10%Ag nanocomposite in a thermal range of 50-700 °C under air atmosphere and its magnetic trait were investigated by thermogravimetric analysis (TGA) and vibrating sample magnetometry (VSM), respectively (Figures S2 and S3, in the SI section). As shown in the TGA curve, proportional to temperature increase, the first shoulder (ca. 10% weight loss) was observed until ca. 280 °C, probably due to the removal of the PVA polymeric network. Then, a gradual weight loss trend was observed until ca. 480 °C, attributed to the dehydration of -OH groups in the PVA strand structure. The fabricated Fe<sub>3</sub>O<sub>4</sub>/PVA-10%Ag nanocomposite exhibited a typical superparamagnetic behavior, as presented in Figure S3. By having this property, the separation process of the nanocatalyst is achieved with high convenience. The magnetic property of the magnetic core is typically reduced proportional to more core coating and new layer creation [25–27]. Accordingly, the M-H curves show that the composition of the PVA polymeric network and Ag NPs causes a reduction in the magnetic property of Fe<sub>3</sub>O<sub>4</sub> NPs. More comprehensive discussion on the TGA and VSM curves is given in the SI section. Brunauer–Emmett–Teller (BET) results are shown in Figures S9-11.

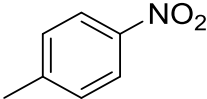
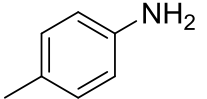
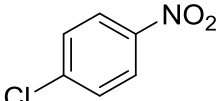
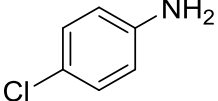
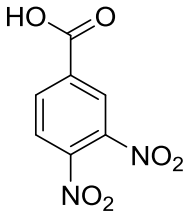
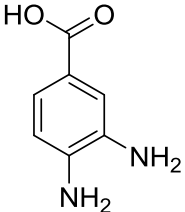
### 2.3. Application

#### 2.3.1. Catalytic activity

To investigate the catalytic efficiency of the produced  $\text{Fe}_3\text{O}_4/\text{PVA-10\%Ag}$  nanocomposite, first, the reaction condition was precisely optimized with various solvents, catalytic ratios, and hydrazine amounts in the reduction reaction of NB (Table 1, entry 1). Detailed information of the optimization process has been reported in Tables S2 and S3, in the SI section. Then, the catalytic activity of the prepared  $\text{Fe}_3\text{O}_4/\text{PVA-10\%Ag}$  nanocomposite was carefully screened using different derivatives of NB, as reported in Table 1. As shown in the table, high reaction yields were obtained when using the  $\text{Fe}_3\text{O}_4/\text{PVA-10\%Ag}$  nanocomposite for short times. However, these results strongly prove the high catalytic performance of the  $\text{Fe}_3\text{O}_4/\text{PVA-10\%Ag}$  nanocomposite when compared with that of other reported catalysts (see Table S4, in the SI section). These values have revealed that  $\text{Fe}_3\text{O}_4/\text{PVA-10\%Ag}$  could be considered as a substantial catalyst for NB reduction reactions. To investigate the effectiveness of the composited  $\text{Fe}_3\text{O}_4$  NPs in terms of catalytic performance, PVA-10%Ag was also applied under the same conditions. According to the Table S2 (entry 11), there was a partial decrease in the obtained yield after removing the  $\text{Fe}_3\text{O}_4$  NPs.

**Table 1.** Obtained yields after the reduction of NB derivatives to aniline derivatives using the  $\text{Fe}_3\text{O}_4/\text{PVA-10\%Ag}$  nanocomposite (30.0 mg), NB (1.0 mmol),  $\text{N}_2\text{H}_4\cdot\text{H}_2\text{O}$  (5.0 mol%), and ethanol (2.0 mL), at 70°C.

Entry	NB structure	Products	Time (min)	Yield <sup>b</sup> (%)	MP (°C)	Ref.
					Found/Reported	
1			5	99	Liquid sample*	[28]
2			15	99	143-145/144-146	[29]
3			7	92	135-140/136.2-138.1	[30]
4			10	94	170-175/171-173	[29]
5			9	93	187-189/186-188	[28]
6			15	89	187-189/185-187	[32]
7			10	96	64-66/65-66	[33]
8			14	90	50-53/52-53	[31]

9			5	97	41-44/42-43	[32]
10			8	97	69-71/70-72	[29]
11			16	89	209-212/208-210	[34]

\*Liquid sample was identified with boiling point screening and thin-layer chromatography (TLC) (bp ca.184 °C)

b: The yields refer to the isolated products.

### 2.3.2. Suggested mechanism

The catalytic role of Ag NPs in the reduction reaction of NB derivatives in the presence of  $N_2H_4 \cdot H_2O$  and a plausible mechanism are illustrated in Figure 3. According to the figure, based on the observed results in the present work and knowledge from earlier precedents, it is believed that effective electronic interactions between Ag and heteroatoms can create an appropriate substrate for this type of reaction [35]. These close electronic interactions of heteroatoms with dissociated hydrogen atoms from hydrazine hydrate, onto the surface of the Ag NPs cause NB derivatives to be adsorbed and converted to anilines during successive dehydration processes. In fact, hydrazine hydrate is considered as a substantial H-supporter for the reduction process and can effectively interact with Ag NPs surfaces from its nitrogen sites.

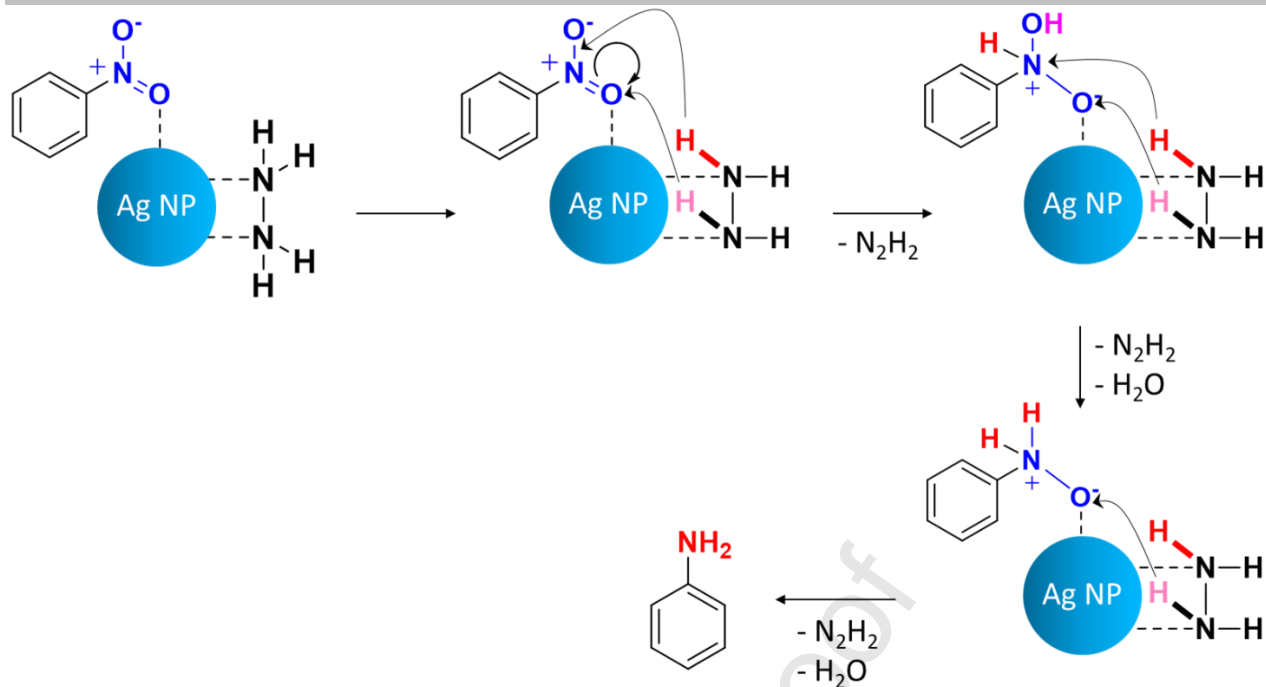


**Figure 3.** A plausible mechanism for the reduction of NB derivatives to anilines using the  $\text{Fe}_3\text{O}_4/\text{PVA}-10\%\text{Ag}$  nanocomposite in the presence of hydrazine hydrate.

### 2.3.3. Recyclability

To monitor the recyclability of the produced  $\text{Fe}_3\text{O}_4/\text{PVA}-10\%\text{Ag}$  hybrid nanocomposite, it was separated from the reaction mixture using an external magnet after completion of the reaction of NB reduction. Then, the particles were washed well several times with ethanol and deionized water, dried, and used again in further reactions. Afterward, they were dispersed well in deionized water by ultrasonication and washed again with ethanol. Finally, they were dried well at  $60\text{ }^\circ\text{C}$ . After recycling and reusing five times, reduction in the reaction yields was observed, probably due to the separation of Ag NPs during the catalytic process (Figure S4, in the SI section).

### 2.3.4. Biological activity

The presented product  $\text{Fe}_3\text{O}_4/\text{PVA}-10\%\text{Ag}$  hybrid nanocomposite could be used for biological applications. This property was achieved through the composition of Ag NPs with  $\text{Fe}_3\text{O}_4$  NPs. Accordingly, we evaluated the antibacterial activity of our desired product by carrying out the *in vitro*

biological tests. The antibacterial properties of the samples toward gram-positive *Staphylococcus aureus* (*S. aureus*, ATCC 12600) and gram-negative *Escherichia coli* (*E. coli*, ATCC 9637) bacteria were evaluated according to the disc diffusion antibiotic sensitivity test. The samples were poured onto the nutrient agar plates cultured with bacterial cells, and then the plates were incubated at 37 °C for 24 h. The antibacterial effects of the Fe<sub>3</sub>O<sub>4</sub>/PVA-10%Ag hybrid nanocomposite were investigated with execution of the zone of the inhibition (ZOI) on *E. coli* and *S. aureus* cells, which show the inhibitory property of microbial growth around the discs (Figure S5 a,b – in the SI section). The antibiotic gentamicin was employed as the positive control in this study. Colony-forming unit (CFU) test was also carried out to monitor the antibacterial activity of Fe<sub>3</sub>O<sub>4</sub>/PVA-10%Ag using *E. coli* and *S. aureus*. As shown in Figure S5 c–f, a large number colonies of *E. coli* and *S. aureus* (images c and d) were reduced by our nanoscale composite product after 24 h (images e and f). The results obtained from the plate count technique are reported in Table 2.

**Table 2.** Results obtained from disk diffusion and CFU tests using the Fe<sub>3</sub>O<sub>4</sub>/PVA-10%Ag nanocomposite.

Sample	ZOI <i>E. coli</i> (mm)	ZOI <i>S. aureus</i> (mm)	P.C ( <i>E. coli</i> )	P.C ( <i>S. aureus</i> )
Gentamicin	6 ± 0.7	7.5 ± 0.8	768 ± 71	644 ± 59
Fe <sub>3</sub> O <sub>4</sub> /PVA-10%Ag	2.22 ± 0.24	3.09 ± 0.22	185 ± 24	48 ± 32

mm: clear area in millimeters, P.C: plate count.

### 3. Experimental

#### 3.1. Materials and devices

All the chemicals and equipment used in this study are reported in the SI section.

#### 3.2. Practical methods

*Preparation of the PVA-coated Fe<sub>3</sub>O<sub>4</sub> NPs*

In a three-necked round-bottom flask (250 mL), polyvinyl alcohol (PVA; 2.0 g, PVA 72000) was dissolved well in 40.0 mL deionized water into an oil bath at 80 °C until a homogeneous mixture was obtained. Then, under N<sub>2</sub> atmosphere, ammonia solution (12.0 mL) was added into the flask and pH was carefully checked with a pH paper (pH~12). Next, a homogeneous yellow solution of FeCl<sub>2</sub>·4H<sub>2</sub>O (1.0 g, 7.9 mmol) and FeCl<sub>3</sub>·6H<sub>2</sub>O (2.5 g, 9.2 mmol) in deionized water (10.0 mL) was added dropwise. After completion of the addition, the solution was stirred continuously for additional 2 h under the same conditions. Afterward, the produced dark magnetic NPs were magnetically collected and washed several times with deionized water and ethanol. Finally, the dark magnetic NPs were dried at 60 °C.

*Preparation of the Fe<sub>3</sub>O<sub>4</sub>/PVA-10%Ag hybrid nanocomposite*

The prepared Fe<sub>3</sub>O<sub>4</sub>/PVA NPs (0.5 g) were initially dispersed well in deionized water (15.0 mL) using an ultrasonic bath. Then, AgNO<sub>3</sub> (1.0 g, 5.9 mmol) was added into the flask and stirred for 4 h at room temperature. Ultimately, the magnetic NPs were collected using an external magnet and washed several times with ethanol and deionized water. The dark brown NPs were dried at 60 °C.

*3.3. Spectral data for selected compounds*

4-Aminophenol (Table 3, Entry 6): white solid, <sup>1</sup>H NMR (500 MHz, DMSO): δ (ppm) = 4.38 (2H, s, NH<sub>2</sub>), 6.42–6.44 (2H, d, J=10 Hz, H–Ar), 6.48–6.50 (2H, d, J=10 Hz, H–Ar), 8.37 (1H, s, OH).

**4. Conclusions**

Among various species of hazardous chemical compounds, NB derivatives are compounds that have to be removed or converted to nontoxic aniline derivatives through convenient strategies. In this regard, one of the most convenient methods is the use of magnetic nanocatalysts, as they have distinguished properties such as magnetic property, extreme surface area, surface-functionalization ability, notable thermal resistance, and nontoxicity. Herein, we introduced an efficient organic–

inorganic hybrid nanocomposite made of iron oxide nanoparticles, PVA strands, and Ag NPs ( $\text{Fe}_3\text{O}_4/\text{PVA}-10\%\text{Ag}$ ) for the reduction of the NB derivatives to their aniline forms. According to the suggested mechanism, Ag NPs, which were loaded onto the surface of PVA-coated iron oxide nanoparticles, are responsible for the catalytic activity of this nanocomposite through their electronic effects with heteroatoms. Additionally, they have added the biological effect to the presented nanocomposite through their antibacterial property. All structural characterization studies such as FT-IR, EDX, XRD, and TGA were performed, and the results obtained were precisely interpreted in the context. Moreover, the magnetic property of the presented nanocatalyst was investigated by VSM analysis, and super-paramagnetic treatment was observed. The morphology, uniformity, and size of the particles were investigated by SEM imaging.

### **Acknowledgments**

The authors gratefully acknowledge the partial support from the Research Council of the Iran University of Science and Technology and the Iran National Science Foundation (INSF).

### **Disclosure statement**

The authors declare no potential conflict of interest.

### **Supplementary data**

Supplementary data can be found in the online version of this article.

## References

1. R. Begum, Z.H. Farooqi, Z. Butt, Q. Wu, W. Wu, A. Irfan, Engineering of responsive polymer based nano-reactors for facile mass transport and enhanced catalytic degradation of 4-nitrophenol, *J. Environ. Sci.* 72 (2018) 43-52.
2. G. Medina-Pérez, F. Fernández-Luqueño, E. Vazquez-Nuñez, F. López-Valdez, J. Prieto-Mendez, A. Madariaga-Navarrete, M. Miranda-Arámbula, Remediating polluted soils using nanotechnologies: Environmental Benefits and Risks, *Pol. J. Environ. Stud.* 28 (2019) 1013–1030.
3. R. Begum, J. Najeeb, G. Ahmad, W. Wu, A. Irfan, A.G. Al-Sehemi, Z.H. Farooqi, Synthesis and characterization of poly (N-isopropylmethacrylamide-co-acrylic acid) microgels for *in situ* fabrication and stabilization of silver nanoparticles for catalytic reduction of o-nitroaniline in aqueous medium, *React. Funct. Polym.* 132 (2018) 89-97.
4. Z.H. Farooqi, R. Khalid, R. Begum, U. Farooq, Q. Wu, W. Wu, M. Ajmal, A. Irfan, K. Naseem, Facile synthesis of silver nanoparticles in a crosslinked polymeric system by in situ reduction method for catalytic reduction of 4-nitroaniline, *Environ. Technol.* 40 (2019) 2027-2036.
5. Z.H. Farooqi, A. Ijaz, R. Begum, K. Naseem, M. Usman, M. Ajmal, U. Saeed, Synthesis and characterization of inorganic–organic polymer microgels for catalytic reduction of 4- nitroaniline in aqueous medium, *Polym. Composite.* 39 (2018) 645-653.
6. R. Begum, Z.H. Farooqi, E. Ahmed, K. Naseem, S. Ashraf, A. Sharif, R. Rehan, Catalytic reduction of 4- nitrophenol using silver nanoparticles- engineered poly (N- isopropylacrylamide- co- acrylamide) hybrid microgels, *Appl. Organomet. Chem.* 31 (2017) 3563.
7. K. Naseem, R. Begum, Z.H. Farooqi, Catalytic reduction of 2-nitroaniline: a review, *Environ. Sci. Pollut. R.* 24 (2017) 6446-6460.
8. R. Begum, R. Rehan, Z.H. Farooqi, Z. Butt, S. Ashraf, Physical chemistry of catalytic reduction of nitroarenes using various nanocatalytic systems: past, present, and future, *J. Nanoparticle Res.* 18 (2016) 231.
9. M. Baron, E. Metay, M. Lemaire, F. Popowycz, Reduction of aromatic and aliphatic nitro groups to anilines and amines with hypophosphites associated with Pd/C, *Green Chem.* 15 (2013) 1006-1015.

10. S. Földner, P. Pohla, H. Bartling, S. Dankesreiter, R. Stadler, M. Gruber, A. Pfitzner, B. König, Selective photocatalytic reductions of nitrobenzene derivatives using  $\text{PbBiO}_2\text{X}$  and blue light, *Green Chem.* 13 (2011) 640-643.
11. P. Piccinini, C. Minero, M. Vincenti, E. Pelizzetti, Photocatalytic mineralization of nitrogen-containing benzene derivatives, *Catal. Today.* 39 (1997) 187-195.
12. A. Maleki, R. Taheri- Ledari, M. Soroushnejad, Surface functionalization of magnetic nanoparticles via palladium- catalyzed Diels- Alder approach, *ChemistrySelect* 3 (2018) 13057-13062.
13. R. Taheri-Ledari, J. Rahimi, A. Maleki. Synergistic catalytic effect between ultrasound waves and pyrimidine-2,4-diamine-functionalized magnetic nanoparticles: Applied for synthesis of 1,4-dihydropyridine pharmaceutical derivatives, *Ultrason Sonochem.* 59 (2019) 104737.
14. S. Rostamnia, B. Zeynizadeh, E. Doustkhah, A. Baghban, K.O. Aghbash, The use of  $\kappa$ -carrageenan/ $\text{Fe}_3\text{O}_4$  nanocomposite as a nanomagnetic catalyst for clean synthesis of rhodanines, *Catal. Commun.* 68 (2015) 77-83.
15. A. Maleki, M. Niksefat, J. Rahimi, Z. Hajizadeh, Design and preparation of  $\text{Fe}_3\text{O}_4$ @PVA polymeric magnetic nanocomposite film and surface coating by sulfonic acid via in situ methods and evaluation of its catalytic performance in the synthesis of dihydropyrimidines, *BMC Chem.* 13 (2019) 19.
16. A. Maleki, J. Rahimi, Z. Hajizadeh, M. Niksefat, Synthesis and characterization of an acidic nanostructure based on magnetic polyvinyl alcohol as an efficient heterogeneous nanocatalyst for the synthesis of  $\alpha$ -aminonitriles, *J. Organomet. Chem.* 881 (2019) 58-65.
17. S. Mallakpour, M. Hatami, An effective, low-cost and recyclable bio-adsorbent having amino acid intercalated  $\text{LDH@Fe}_3\text{O}_4$ /PVA magnetic nanocomposites for removal of methyl orange from aqueous solution, *Appl. Clay. Sci.* 174 (2019) 127-137.
18. S. Ashraf, R. Begum, R. Rehan, W. Wu, Z.H. Farooqi, Synthesis and characterization of pH-responsive organic-inorganic hybrid material with excellent catalytic activity, *J. Inorg. Organomet. P.* 28 (2018) 1872-1884.
19. M. Shahid, Z.H. Farooqi, R. Begum, K. Naseem, M. Ajmal, A. Irfan, Designed synthesis of silver nanoparticles in responsive polymeric system for their thermally tailored catalytic activity towards hydrogenation reaction, *Korean. J. Chem. Eng.* 35 (2018) 1099-1107.
20. R. Begum, Z.H. Farooqi, A.H. Aboo, E. Ahmed, A. Sharif, J. Xiao, Reduction of nitroarenes catalyzed by microgel-stabilized Ag nanoparticles, *J. Hazard. Mater.* (2019).

21. S.R. Khan, Z.H. Farooqi, A. Ali, R. Begum, F. Kanwal, M. Siddiq, Kinetics and mechanism of reduction of nitrobenzene catalyzed by silver-poly (N-isopropylacryl amide-co-allylactic acid) hybrid microgels, *Mater. Chem. Phys.* 171 (2016) 318-327.
22. N. Anbu, C. Vijayan, A. Dhakshinamoorthy, A versatile, mild and selective reduction of nitroarenes to aminoarenes catalyzed by CeO<sub>2</sub> nanoparticles with hydrazine hydrate, *ChemistrySelect.* 4 (2019) 1379-1386.
23. A. Maleki, M. Niksefat, J. Rahimi, S. Azadegan, Facile synthesis of tetrazolo [1,5-a] pyrimidine with the aid of an effective gallic acid nanomagnetic catalyst, *Polyhedron* 167 (2019)103-110.
24. A. Maleki, M. Kamalzare, Fe<sub>3</sub>O<sub>4</sub>@cellulose composite nanocatalyst: Preparation, characterization and application in the synthesis of benzodiazepines, *Catal. Commun.* 53 (2014) 67-71.
25. A. Maleki, R. Taheri-Ledari, J. Rahimi, M. Soroushnejad, Z. Hajizadeh, Facile Peptide Bond Formation: Effective Interplay between Isothiazolone Rings and Silanol Groups at Silver/Iron Oxide Nanocomposite Surfaces, *ACS Omega* 4 (2019) 10629-10639.
26. A. Maleki, M. Niksefat, J. Rahimi, R. Taheri-Ledari, Multicomponent synthesis of pyrano[2,3-d]pyrimidine derivatives via a direct one-pot strategy executed by novel designed copperated Fe<sub>3</sub>O<sub>4</sub>@polyvinyl alcohol magnetic nanoparticles, *Mater. Today Chem.* 13 (2019) 110-120.
27. A. Maleki, R. Taheri-Ledari, R. Ghalavand, R. Firouzi-Haji, Palladium-decorated o-phenylenediamine-functionalized Fe<sub>3</sub>O<sub>4</sub>/SiO<sub>2</sub> magnetic nanoparticles: A promising solid-state catalytic system used for Suzuki-Miyaura coupling reactions, *J. Phys. Chem. Solids* 136 (2020) 109200.
28. V. Kandathil, T.S. Koley, K. Manjunatha, R.B. Dateer, R.S. Keri, B.S. Sasidhar, S.A. Patil, S.A. Patil, A new magnetically recyclable heterogeneous palladium (II) as a green catalyst for Suzuki-Miyaura cross-coupling and reduction of nitroarenes in aqueous medium at room temperature, *Inorganica Chim. Acta.* 478 (2018) 195-210.
29. R. Mirbagheri, D. Elhamifar, Magnetic ethyl-based organosilica supported Schiff-base/indium: A very efficient and highly durable nanocatalyst, *J. Alloys Compd.* 790 (2019) 783-791.
30. Z. Hu, Y. Ai, L. Liu, J. Zhou, G. Zhang, H. Liu, X. Liu, Z. Liu, J. Hu, H.B. Sun, Q. Liang, Hydroxyl assisted rhodium catalyst supported on goethite nanoflower for chemoselective catalytic transfer hydrogenation of fully converted nitrostyrenes, *Adv. Synth. Catal.* 361 (2019) 3146-3154.

31. T. Maejima, Y. Shimoda, K. Nozaki, S. Mori, Y. Sawama, Y. Monguchi, H. Sajiki, One-pot aromatic amination based on carbon–nitrogen coupling reaction between aryl halides and azido compounds, *Tetrahedron*, 68 (2012) 1712-1722.
32. S. Sobhani, F.O. Chahkamali, J.M. Sansano, A new bifunctional heterogeneous nanocatalyst for one-pot reduction-Schiff base condensation and reduction–carbonylation of nitroarenes, *RSC Adv.* 9 (2019) 1362-1372.
33. M. Rajabzadeh, H. Eshghi, R. Khalifeh, M. Bakavoli, Generation of Cu nanoparticles on novel designed Fe<sub>3</sub>O<sub>4</sub>@SiO<sub>2</sub>/EP. EN. EG as reusable nanocatalyst for the reduction of nitro compounds, *RSC Adv.* 6 (2016) 19331-19340.
34. J. Li, E.D. Inutan, B. Wang, C.B. Lietz, D.R. Green, C.D. Manly, A.L. Richards, D.D. Marshall, S. Lingenfelter, Y. Ren, S. Trimpin, Matrix assisted ionization: new aromatic and nonaromatic matrix compounds producing multiply charged lipid, peptide, and protein ions in the positive and negative mode observed directly from surfaces, *J. Am. Soc. Mass. Spectr.* 23 (2012) 1625-1643.
35. M.B. Gawande, H. Guo, A.K. Rathi, P.S. Branco, Y. Chen, R.S. Varma, D.L. Peng, First application of core-shell Ag@Ni magnetic nanocatalyst for transfer hydrogenation reactions of aromatic nitro and carbonyl compounds. *RSC Adv.* 3 (2013) 1050-1054.

## Competing interests statement

The authors whose names are listed in this article have no competing interests in this paper.

Journal Pre-proof

**Highlights**

---

- $\text{Fe}_3\text{O}_4/\text{PVA}-10\%\text{Ag}$  is presented a novel, efficient and recyclable magnetic nanocomposite.
- Uniform and spherical shape nanoparticles in the mean size 21 nm have been prepared.
- Versatile nanocomposite with high catalytic and biological activities is introduced.
- Reduction of nitrobenzenes have been done in short reaction times.
- Synergistic magnetic effect between Ag and  $\text{Fe}_3\text{O}_4$  nanoparticles has been investigated.

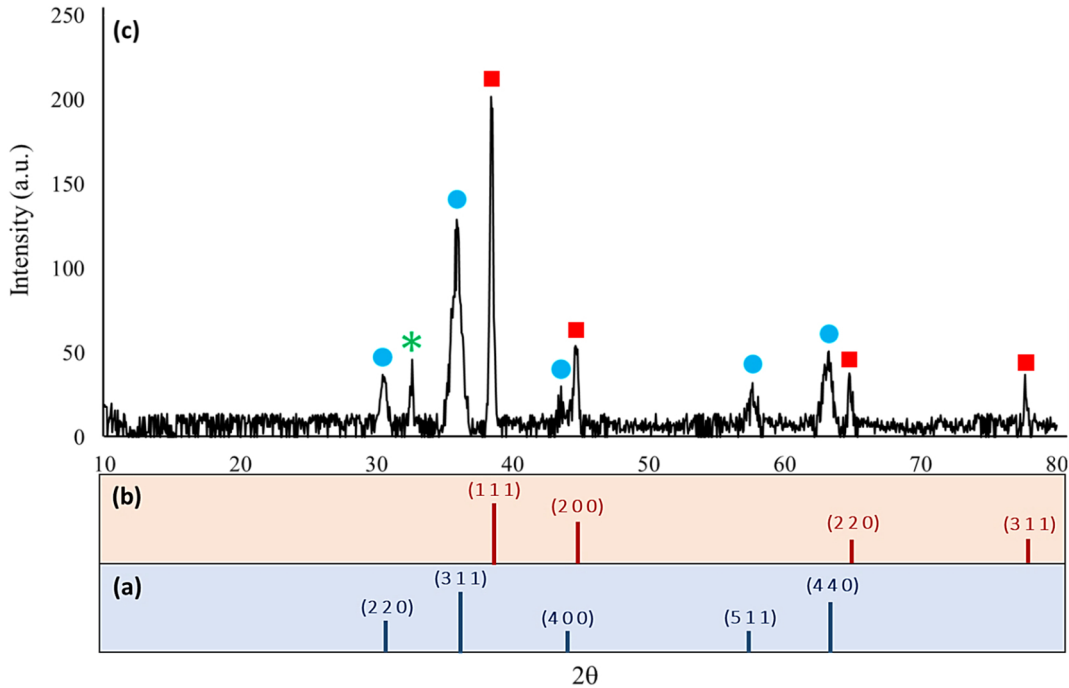


Figure 1

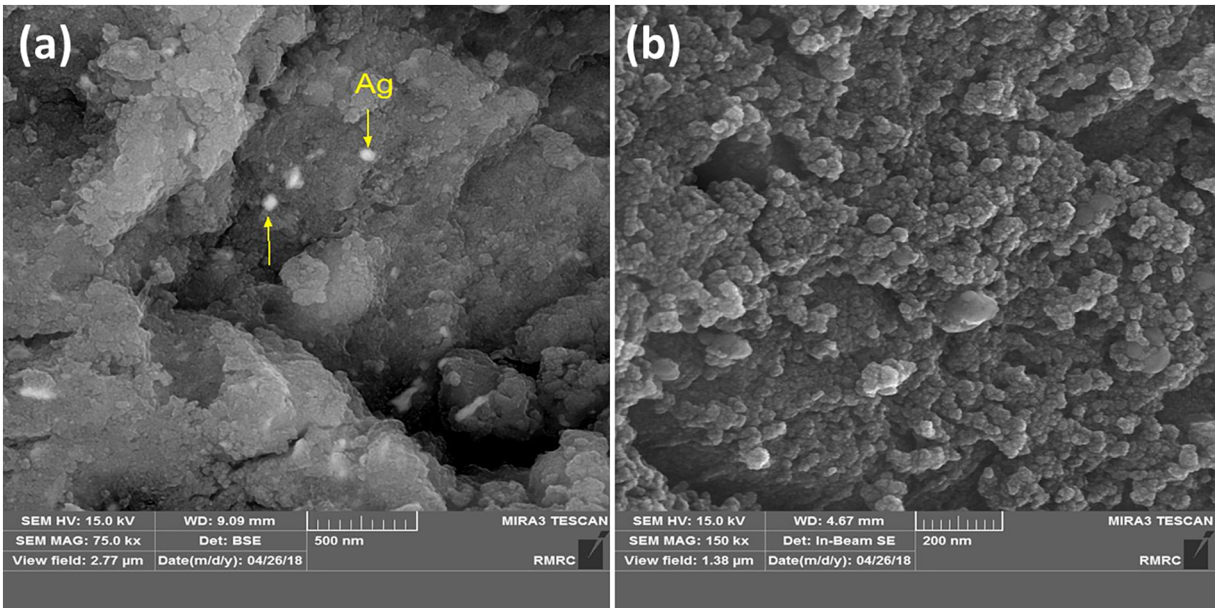


Figure 2

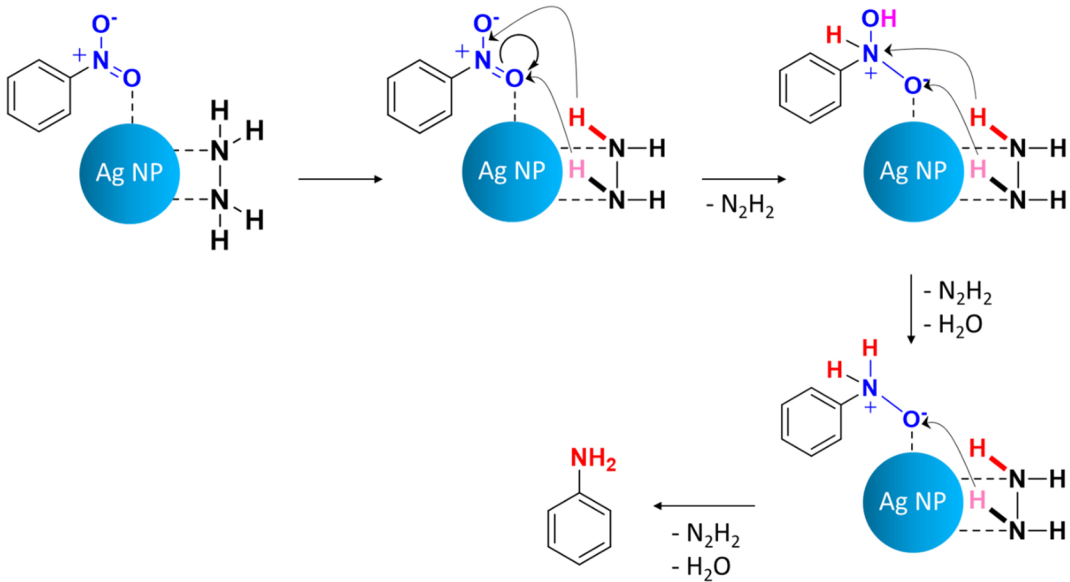


Figure 3